# Chapter 14

## Summary and Conclusions

**ZhongPing Lee, Ronald Zaneveld, Stephane Maritorena, Hubert Loisel, Roland Doerffer, Paul Lyon, Emmanuel Boss, Kendall Carder, Emmanuel Devred and Robert Arnone**

Most algorithms used in ocean colour remote sensing attempt to derive, directly, the concentrations of water constituents, mainly phytoplankton chlorophyll concentration. In this report, however, we present and discuss algorithms which have been developed to derive inherent optical properties (IOPs) from water-leaving radiance, in a one-step or multi-step process. The IOPs are then decomposed into the contributions by different optical components, such as absorption by phytoplankton pigments, and finally the IOPs of different components are converted into concentrations.

IOPs are the fundamental parameters of hydrological optics. The IOPs, in combination with radiances from the sun and sky, determine water-leaving radiance, which in turn defines water colour (an apparent optical property). At the same time, IOPs are also environmental properties. Their variations are directly related to changes in concentration, size distribution and composition of particulate matter and/or dissolved constituents. IOPs derived from remote sensing of ocean colour provide innovative opportunities for environmental observation and oceanographic studies on time and space scales not achievable with *in situ* measurements.

To derive, accurately, various IOPs from water colour, as presented here, is not a simple task. This report presents some frequently encountered methods for IOP retrieval. These algorithms have different levels of complexity; some are explicit about all elements and derivation processes, some are implicit; some have fewer empirical inputs, while others have more empiricism built into them. Table 14.1 highlights their similarities and major characteristics.

When presenting and comparing models, it is always useful to remember that models, by their very nature, represent some sort of reduction, or simplification. It naturally follows that practically all models will have some limitation when they attempt to mimic nature. Thus there is often a need to tailor models for specific applications or for specific regions. If models are applied for purposes for which they were not designed, there is always a risk of poor per-

**Table 14.1** Algorithm highlights. L98 - Spectral-ratio algorithm (Lee *et al.* 1998, Chapter 4); B99 - Spectral curvature algorithm (Barnard *et al.* 1999, Chapter 4); MM01 - Spectral-ratio algorithm (Morel and Maritorena, 2001, Chapter 4); Loisel - Inversion of IOP (Chapter 5); D&S - MERIS Neural Network Algorithm (Chapter 6); Lyon - Linear Matrix Inversion (Chapter 7); Boss - Over constrained Linear Matrix Inversion (Chapter 8); Carder - MODIS semi-analytical algorithm (Chapter 9); QAA - Quasi-Analytical Algorithm (Chapter 10); GSM - Garver, Siegel and Maritorena semi-analytical model (Chapter 11); SPD - Sathyendranath, Platt and Devred semi-analytical reflectance model (Chapter 12).

| **Algorithm** | **Type** | **Key features** |
|---|---|---|
| L98 | Empirical | Empirical constants; products at 440 nm only |
| B99 | Semi-empirical | Relationships between total absorption coefficients |
| MM01 | | Bio-optical models; hyperspectral |
| Loisel | | $K_d(\lambda)$ from $R_{rs}(\lambda)$ empirically |
| D&S | Neural Network | Neural constants; MERIS only |
| Lyon | Algebraic *(Linear Matrix Inversion)* | Spectral models for $a_{ph}(\lambda)$, $a_{dg}(\lambda)$, and $b_{bp}(\lambda)$ |
| Boss | | Varying spectral shapes for $a_{ph}(\lambda)$, $a_{dg}(\lambda)$, and $b_{bp}(\lambda)$; statistical selection of solution; generates output confidence intervals; applicable to multi- and hyperspectral data |
| Carder | Algebraic for low absorption waters (*iterative solution*); empirical for other | Spectral models for $a_{ph}(\lambda)$, $a_{dg}(\lambda)$, and $b_{bp}(\lambda)$; empirical coefficients for different properties |
| QAA | Algebraic | Separate derivations for the total and individual components; spectral models for $a_{dg}(\lambda)$ and $b_{bp}(\lambda)$; retrieve multi- or hyperspectral $a_{ph}$ spectrum |
| GSM | Spectral optimization | Optimized spectral shapes for $a_{ph}(\lambda)$, $a_{dg}(\lambda)$, and $b_{bp}(\lambda)$; applicable to multi- and hyperspectral data; can use input uncertainties and generates output confidence intervals |
| SPD | | Varying spectral shapes for $a_{ph}(\lambda)$, $a_{dg}(\lambda)$, and $b_{bp}(\lambda)$; applicable to multi- and hyperspectral data |

formance. Thus a golden rule in application of algorithms (and algorithms are a type of model) is to test them always for the specific application or region envisaged, before routine use is made of the algorithm. But knowledge of the features of the model would often help in making the initial selection of an algorithm for a particular application. For example, it is often useful to know if a particular algorithm is non-linear or not; if it is purely empirical or if it is based on theoretical considerations; if it is multi-variable or not; if it is computationally demanding or not. Such relevant features of the algorithms presented in this report are shown in Table 14.1 and Figures 14.1 - 14.4. But, as is often the case with summary tables and figures, they do not represent the whole story, but merely highlight some emergent properties when all models were made as

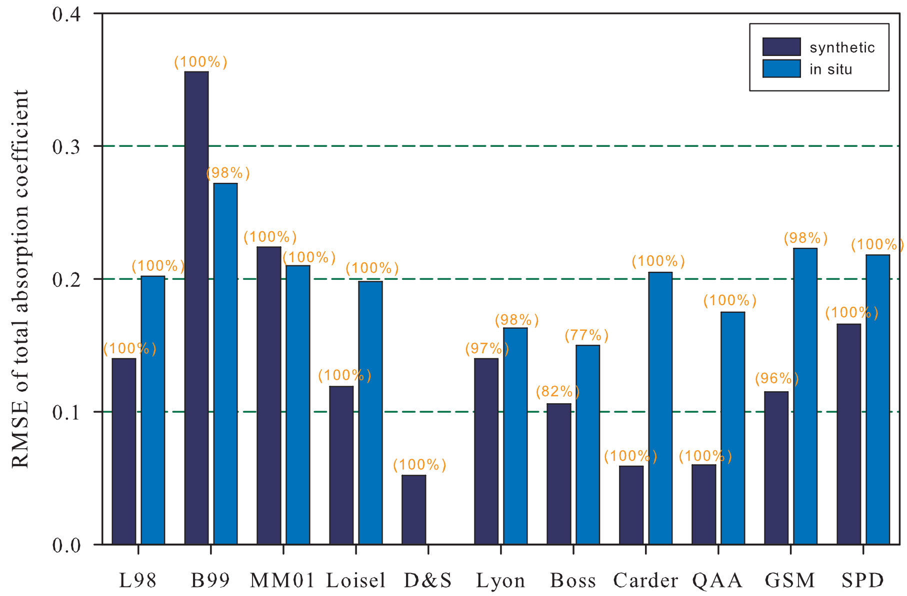


**Figure 14.1** RMSE values for total absorption coefficient of both synthetic and *in situ* data sets, for all algorithms tested (see Table 14.1 for notation of algorithms). The "Lyon" results are for 410 nm, while all other results are in the vicinity of 442 nm. Numbers in parenthesis indicate percentage of valid retrievals for each algorithm. Invalid retrievals are excluded from the calculation of RMSE and other statistical analyses.

comparable as possible, for the purpose of this report.

The RMSE errors presented in Figures 14.1 - 14.4 not only represent the performance of each algorithm, but show also the deviation of the bio-optical model behind each algorithm, from that of the bio-optical model used to prepare the synthetic data set. In addition, the RMSE errors for the *in situ* data set include uncertainties associated with field measurements. It should be noted that not all the algorithms tested used the same number of spectral bands, and some algorithms used fewer bands than what they can potentially use (especially for the synthetic data set).

An inversion algorithm works as a mathematical filter analagous to physical or chemical filters used in the lab or field. In this filtering process, uncertainties are introduced, explicitly or implicitly, into the desired products. More uncertainties are introduced when fewer parameters are under control. Clearly, the results of the various algorithms indicate that there remains room for improvement in the derivation of IOPs from ocean colour. As new information becomes available, it is anticipated that the present algorithms could be revised, or exciting new methods could be developed. It is natural that algorithm development is always a continuing and evolving process.

Nevertheless, we can safely draw the following conclusions based on the

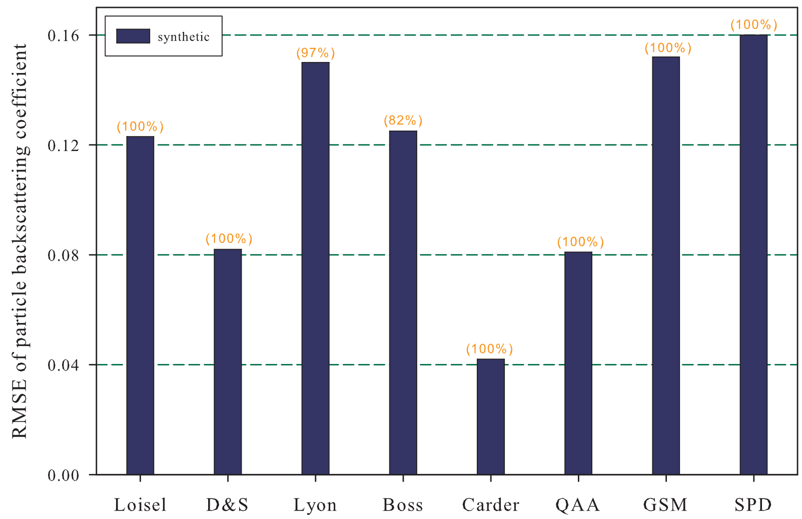


**Figure 14.2** As Fig. 14.1, but for particle backscattering coefficient (synthetic data set only).

presentations and discussions of the various algorithms:

1. In general, the best properties that can be obtained from ocean-colour data, regardless of the algorithm used (see Figures 14.1 to 14.4) and as expected from the inversion of radiative transfer (see Figure 1.3), are the spectral absorption and backscattering coefficients of the total water volume.
2. Using the synthetic data set as a reference (the *in situ* data set prevents the separation of algorithm error from measurement error), more reliable results are obtained for clearer waters ($a(440) < \sim 0.3\ \mathrm{m}^{-1}$). Due to limitations of algorithm architecture and availability of reliable remote-sensing reflectance at specified wavelengths, less accurate results are generally obtained for more absorbing waters ($a(440) > \sim 0.3\ \mathrm{m}^{-1}$).
3. When decomposing the total absorption coefficient into the components of phytoplankton and coloured material, less accurate results (see Figures 14.3 and 14.4) are anticipated due to overlapping of spectral signals and because the spectral shapes of the components are not constant.
4. If the chlorophyll-a concentration ($C$) is desired from ocean colour, more uncertainties will be introduced because the chlorophyll-specific absorption coefficient is not constant at a given wavelength, nor is the relationship between backscattering and chlorophyll well defined.
5. Because there are more unknown factors that affect the retrieval of $C$ from ocean colour than there are unknown factors that affect the retrieval of absorption and backscattering coefficients, we should revisit the issue of $C$ remaining the primary product of ocean-colour remote sensing, rather than the IOPs of the bulk water or the optical properties of phytoplankton.

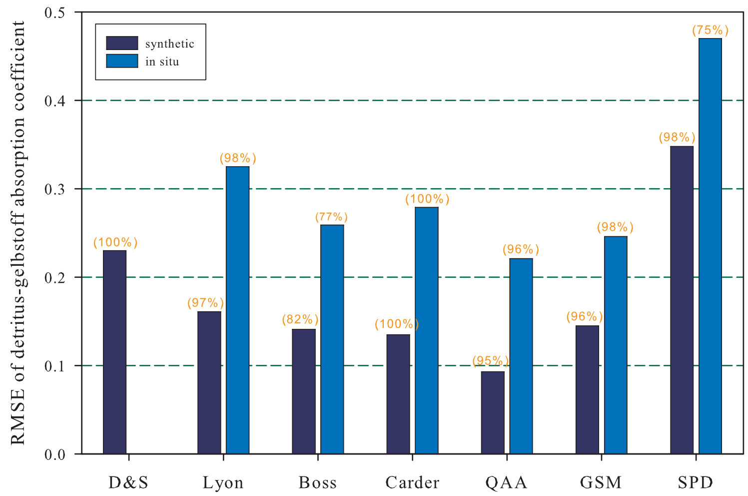


**Figure 14.3** As in Figure 14.1, but for absorption coefficient of detritus and gelbstoff combined.

6. The robust and stable results of the total absorption and backscattering coefficients from these various algorithms (again using the synthetic data set as reference), which were developed independently and are based on different principles, clearly indicate that these optical properties should be taken as standard products for all ocean-colour satellite missions. These optical properties, similar to the sea surface temperature, could serve as climatology data records to study long-term changes of the global oceans.
7. Space-based sensors should be equipped with at least one spectral band in the region of 620-640 nm. Such a band is very important for coastal remote sensing (or for more turbid waters), and algorithm performance would be improved when such a band is included in the process.
8. Algorithms based on the fundamentals of hydrological optics are strongly advocated. Simple empirical relationships prevent understanding of the basics and, therefore, limit advancement in ocean-colour remote sensing. On the other hand, analytical or semi-analytical algorithms enable opportunities to trace back the error sources.

Because inherent optical properties provide important indices for our water environments and open new doors for oceanographic studies, we should spend a great deal of effort on the following issues to improve IOP products:

❖ Increased high-quality, co-located measurements of remote-sensing reflectance and IOPs.

❖ Improved methods to select model parameters such as the spectral shapes of individual IOPs that include $b_b(\lambda)$, $a_{ph}(\lambda)$ and $a_{dg}(\lambda)$. Separation of the global ocean into dynamic biogeochemical provinces may provide vital help in this regard (see IOCCG working group on "Global Ecological Provinces"

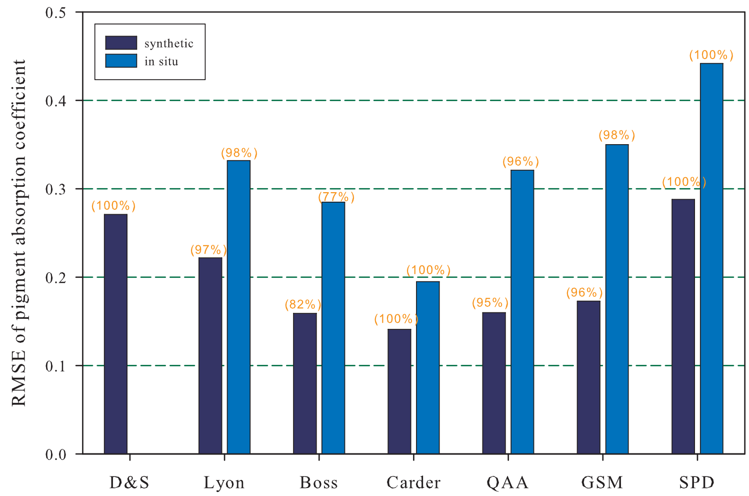


**Figure 14.4** As in Figure 14.1, but for the absorption coefficient of phytoplankton pigments.

http://www.ioccg.org/groups/dowell.html for more information).

- Better quantification of uncertainties in derived products. An in-depth analysis of error sources and their propagation are highly desirable in this regard.
- Improved procedure for atmospheric correction. All algorithms tested use remote-sensing reflectance ($R_{rs}$) as inputs for the calculation of IOPs. Quality of $R_{rs}$, which is one of the products derived from atmospheric correction, plays a critical role in the accuracy of retrieved IOPs. Addition of UV-a bands would assist in the derivation of $R_{rs}$ from satellite measured radiance, especially for coastal waters. Also, such bands may increase the ability to separate phytoplankton absorption from that of dissolved and non-pigmented particulate materials.
- And, finally, enhance and broaden applications of IOPs for oceanographic studies, which are the ultimate goal of ocean-colour remote sensing.

It should be pointed out that in this exercise, the water column was assumed to be homogeneous in terms of its optical properties. Passive optical remote sensing becomes quite a challenge when the optical properties of the upper water column are significantly stratified. Furthermore, we did not touch on issues related to optically shallow environments in this report (for discussions on this issue see IOCCG Report 3). To resolve these important issues, we need to effectively combine measurements from satellite with those from other observatory platforms, such as LIDAR, gliders, and the Network of Coastal Observatories.